Current Research in Food Science 10 (2025) 101056

Contents lists available at ScienceDirect

Current Research in Food Science

journal homepage: www.sciencedirect.com/journal/current-research-in-food-science

The effect of minor components on canola oil oxidation: Oxidation kinetics explained by molecular interactions

Daniel Golodnizky [a], Emil Eshaya [a], Carlos E.S. Bernardes [b,*], Maya Davidovich-Pinhas [a,c,**]

[a] Faculty of Biotechnology and Food Engineering, Technion – Israel Institute of Technology, Haifa, 3200003, Israel
[b] Centro de Química Estrutural, Institute of Molecular Sciences, Departamento de Química e Bioquímica, Faculdade de Ciências, Universidade de Lisboa, 1749-016, Lisboa, Portugal
[c] Russell-Berrie Nanotechnology Institute, Technion – Israel Institute of Technology, Haifa, 3200003, Israel

ARTICLE INFO

Handling Editor: Professor A.G. Marangoni

Keywords:
Minor components
Edible oil
Oxidation
Reverse micelles
MD simulations
Self-assembly

ABSTRACT

This study investigates the effect of various minor components (MCs) on the oxidation kinetics and molecular self-assembly in stripped canola oil during thermal and photo oxidation processes using experimental and simulation tools. The peroxide value (PV) and fatty acid content were measured to evaluate the formation of oxidation products and the consumption rate of unsaturated fatty acids. In the thermal oxidation experiment, adding MCs slightly increased the oxidation rate, while in the photo oxidation experiment, stearic acid (SA) and glycerol monostearate (GMS) significantly decreased it. GMS demonstrated a pronounced ability to self-assemble and form molecular organizations during photo oxidation, resulting in lower critical micelle concentration (CMC) values of lipid hydroperoxides (LOOHs) and reduced oxidation rates. These GMS self-assemblies seem to scatter light, thus decreasing absorbed energy during photo oxidation, leading to lower oxidation rates. SA exhibited the highest surface activity, effectively lowering the LOOH CMC and facilitating the formation of stable reverse micelles at lower concentrations. Interestingly, the addition of MCs did not influence the tendency of LOOHs to form hydrogen bonds with water, suggesting that the lower CMC resulted from the formation of mutual reverse micelles of MCs and LOOHs. Meso-phase formation was observed at very high PVs, indicating a high concentration of secondary oxidation products, which also possess surface activity. These findings underscore the importance of molecular interactions in oxidation stability, providing insights for improving edible oil preservation.

1. Introduction

Vegetable oils contain high amounts of unsaturated fatty acids (USFAs), making these oils beneficial to human diet but susceptible to oil oxidation. In addition to the triacylglycerols that are formed by these USFAs, crude vegetable oils also contain a variety of minor components (MCs), such as traces of water, free fatty acids (FFAs), monoacylglycerols (MAGs), diacylglycerols, phospholipids, pigments, and sterols. To improve oil flavor, appearance, and stability, crude vegetable oils undergo a refining process in which such MCs are mostly removed (Chen et al., 2011a). The refining process improves oil oxidation stability but does not eliminate it due to the high USFAs content. Therefore, the retardation of lipid oxidation in edible oils draws major interest within the scientific and industrial sectors.

The cascade of reactions involved in edible oil oxidation, including the initiation, propagation, and termination phases, has been widely studied (Chaiyasit et al., 2007a; Budilarto and Kamal-Eldin, 2015; Brodnitz, 1968). In recent years, the research focus has shifted to the molecular organizations in bulk oil, which have been established as playing a major role in oxidation kinetics (Chen et al., 2011a; Wang et al., 2024). Such structures are mainly formed due to the presence of traces of water, originating from the plant seed, the refining process, water absorption from the atmosphere, and formation during the oxidation process (Budilarto and Kamal-Eldin, 2015). Therefore, the

* Corresponding author. Centro de Química Estrutural, Institute of Molecular Sciences, Departamento de Química e Bioquímica, Faculdade de Ciências, Universidade de Lisboa, Lisboa, Portugal.
** Corresponding author. The lab of Food Materials Engineering, Faculty of Biotechnology and Food Engineering, Technion Israel institute of Technology, Haifa, Israel.
E-mail addresses: cebernardes@ciencias.ulisboa.pt (C.E.S. Bernardes), dmaya@bfe.technion.ac.il (M. Davidovich-Pinhas).

https://doi.org/10.1016/j.crfs.2025.101056
Received 15 March 2025; Received in revised form 14 April 2025; Accepted 22 April 2025
Available online 23 April 2025

bulk oil can be treated as a micro- or nano emulsion, in which the water molecules are arranged in small droplets forming associated colloids. These associated colloids act like nanoscale reactors that increase the interactions between surface-active molecules, oxidation products, and prooxidant molecules, thus dramatically affecting the oil oxidation stability (Wang et al., 2024; Jalali-Jivan et al., 2020). Such an effect was demonstrated by Kittipongpittaya et al. (2016), who showed that addition of water can either improve or deteriorate the oxidation stability of stripped corn oil, depending on the presence of different surface-active molecules.

Lipid hydroperoxides (LOOHs), which are the primary oxidation products, are amphiphilic molecules that possess surface activity, enabling them to self-assemble at the water-oil interface and form reverse micelles (Ghnimi et al., 2017). Below their critical micelle concentration (CMC), LOOHs are expected to be homogeneously dispersed in the bulk oil. Due to their low concentration and specifically in the vicinity of the water molecules, the probability of LOOHs reacting with prooxidant molecules, which are mainly water-soluble, is low. Therefore, during the period when the LOOHs concentration is below their CMC, termed the induction or the lag period, the oil is considered safe for consumption (Farhoosh, 2018; Golodnizky et al., 2025). Above their CMC, the LOOHs are mostly located at the water-oil interface and are thus expected to be much closer to the water-soluble prooxidant molecules, thereby increasing their reaction rate and consequently accelerating the oxidation rate. Therefore, it has been suggested that the formation of such associated colloids is responsible for the transition from a zero-order oxidation reaction to a first-order reaction, accelerating oil oxidation (Farhoosh, 2018). Moreover, during the oxidation process, the concentrations of water, LOOHs, and secondary products, all of which possess surface activity, increase. This leads to the growth of existing colloids and the formation of new ones. Consequently, the increased number of these associated colloids further accelerates the oxidation rate (Budilarto and Kamal-Eldin, 2015; Jo and Lee, 2021).

The molecular composition in the oil-water interface plays a crucial role in oil oxidation kinetics and oil stability. Oil MCs possess surface activity and are expected to accumulate at the oil-water interface. Their accumulation on this interface has been shown to impact the reactivity of oxidation products with prooxidant and antioxidant molecules, consequently affecting the oxidation rate (Chen et al., 2011a). Phospholipids, one of the extensively studied surface active oil MCs, are distinguished by their large polar groups, typically resulting in a medium hydrophilic-lipophilic balance (HLB) value of approximately 8. This characteristic enables them to form micelles in both polar and nonpolar solvents (Cui et al., 2014). The impact of reverse micelle formation of some phospholipids, such as 1,2-dioleoyl-sn-glycero-3-phosphocholine (DOPC) and 1,2-dioleoyl-sn-glycero-3-phosphoethanolamine (DOPE), was previously demonstrated (Cui et al., 2014). It was shown that both phospholipids, below their CMC, did not affect the oxidation stability of stripped soybean oil, while above it, they had a prooxidant activity. Such prooxidant activity was related to their ability to form reverse micelles, in which the oxidation reactions are accelerated. Moreover, it was shown that a combination of DOPC above its CMC with antioxidants had different effects on antioxidant activity. At the lower concentration, DOPC enhanced the antioxidant activity and improved the oil oxidation stability. On the other hand, at the higher concentration, it reduced the antioxidant activity, thus deteriorating oil oxidation stability. Such effects were also dependent on the antioxidant polarity, where the more polar Trolox was more affected compared with the less polar α-tocopherol due to their involvement in the interfacial stabilization (Chen et al., 2011b). These observations were explained by the ability of phospholipids to affect the molecular composition at the water-oil interface, which is directly related to the oxidation kinetics.

Other surface-active MCs, such as FFAs, diacylglycerols, and MAGs, have much smaller polar groups, resulting in HLB values of about 1, 1.8, and 3.4–3.8, respectively (Wang et al., 2024). These HLB values allow them to accumulate at the water-oil interface of the reverse micelles formed during the oxidation process, thus their presence is expected to affect oxidation stability. The typical FFA composition in a commercially refined oil is about 0.1 %wt. and gradually increases during storage (Chen et al., 2011a). At this typical concentration range, which is below the FFA CMC, the formation of reverse micelles formed solely by FFAs is unlikely (Paradiso et al., 2018; Kittipongpittaya et al., 2014). However, in the presence of other surface-active molecules, such as DOPC, the FFAs can join the existing colloids and affect their properties. In the study by Kittipongpittaya et al. (2014), it was shown that addition of oleic acid (OA) to stripped oil containing DOPC shortened the lag period, resulting in a decrease in oil oxidation stability. This phenomenon was explained by the lower pH of the water droplets measured in the presence of OA at the water-oil interface. Such a lower pH was suggested to accelerate the LOOHs acid-catalyzed decomposition, leading to higher propagation reaction rates. Moreover, it was suggested that the presence of OA in the oil-water interface can attract transition metals, thus bringing them closer to the LOOHs and accelerating the oxidation process (Kittipongpittaya et al., 2016). It was also shown that OA can interact with LOOHs and alter their reverse micelle shape and size (Chaiyasit et al., 2007b). Other oil MCs, such as stearyl alcohol (SO) and a mixture of MAGs, were also shown to play a role in the interface molecular composition, thus affecting oil stability and α-tocopherol antioxidant activity (Kortenska et al., 2002; Delfanian et al., 2023). All these examples demonstrate the importance of understanding the molecular composition of the water-oil interface while considering oil oxidation stability.

To achieve a deep understanding of the interactions between surface-active molecules, water molecules, and oxidation products, molecular resolution is required. A common tool that provides such resolution is molecular dynamics (MD) simulation, in which atomic and molecular interactions are computed to monitor the movement of model systems of interest (Golodnizky et al., 2022, 2023; Smith, 2022; Chen et al., 2021). In the field of lipid oxidation, the most explored systems are phospholipidic membranes, which are studied to evaluate the effect of oxidation on cell membrane properties such as shape, permeability, and fluidity (Siani et al., 2016; Agmon et al., 2018; Yadav et al., 2019). While the effect of phospholipids on oil oxidation is extensively studied, there is not much research addressing other oil MCs surface activity and their effect on oil stability. In our recent work, we examined the interaction tendency of typical photo and thermal LOOHs to self-assemble under photo and thermal conditions, and the effect of these molecular organizations on oxidation kinetics using experimental and simulation tools. We showed that the tendency to form hydrogen bonds between the water molecules and the thermal LOOHs was higher than that of the photo LOOHs, leading to lower thermal LOOH CMC. Such a lower CMC led to a higher oxidation rate in the thermal oxidation experiment, which was also positively correlated with temperature (Golodnizky et al., 2025).

In the current research, MD simulations were applied to study the molecular interactions of oil MCs, water molecules, and LOOHs, to achieve a deep understanding of their tendency to self-assemble at the water-oil interface. Moreover, this computational method was combined with experimental methods to explore how these self-assemblies affect the oxidation kinetics. More specifically, canola oil was introduced, using its two most abundant triacylglycerols (TAGs), triolein (OOO) and 1,3-dioleoyl-2-linoleoyl (OLiO) (Neff et al., 1994), and water. The oxidation primary products, 1,3-dioleoyl-2-(9-hydroperoxy-10E,12E-octadecadienoyl)-sn-glycerol(1,3-OO-2-(9-EE-HpODE)-TAG) (abbreviated as 9EEH-pODE in the current study) and 1,3-dioleoyl-2-(12-hydroperoxy-9z, 13E-octadecadienoyl)-sn-glycerol(1,3-OO-2-(12-HpODE)-TAG) (abbreviated as 12HpDOE in the current study), which are oxidized forms of OLiO, were included in the model as typical thermal and photo oxidation LOOHs, respectively (Kato et al., 2018). Additionally, the oil MCs, SO, stearic acid (SA), and glycerol monostearate (GMS), were introduced, all containing 18-carbons alkyl chains and different polar head groups. SO has only a hydroxyl group, giving it the lowest polarity, while GMS contains a bulky

glycerol group with an ester bond and two hydroxyl groups, resulting in the highest polarity (Fig. 1). While monoglycerides and FFAs are naturally present in edible oils at concentrations of around 0.1 % w/w, which may vary during storage (Chen et al., 2011a; Flickinger and Matsuo, 2003), fatty alcohols are found only in trace amounts. Their inclusion in this study was therefore driven more by systematic considerations than by practical relevance. These molecules were selected to examine the effect of their polar head groups on the formation of association colloids and their influence on oil oxidation kinetics. It is worth noting that other type of molecules, such as phospholipids and tocopherols, also affect oil oxidation but were beyond the scope of the current study. Such model allowed us to study the molecular interactions between the different MCs, the oxidation products, and the water molecules, and in combination with experimental techniques, to evaluate the effect of such interactions on oil oxidation stability.

2. Materials and methods

2.1. Materials

Canola oil was purchased from the local supermarket (private label Shufersal). Glycerol monostearate (GMS) purified (>95 %), 1-Octadecanol (SO) (99 %), and ammonium thiocyanate (>99 %), were purchased from Thermo Scientific Chemicals (Holland Moran, Israel). Chloroform Reagent ACS Spectro Grade (99.8 %), Methanol RS SPECTROSOL for optical spectroscopy were purchased from Thermo Scientific Chemicals and CARLO ERBA Reagents, respectively. Iron (II) chloride tetrahydrate and Iron (III) chloride 6 hydrate were purchased from EMSURE and Honeywell respectively (Holland Moran, Israel). Methyl FA esters (FAMEs) standard mixture (25 FAME mixture) was purchased from United states pharmaceuticals (USP) (Holland Moran, Israel). Hydrochloric acid (32 %), potassium hydroxide (KOH), and n-Hexane were purchased from Bio-Lab ltd. Stearic acid (SA) (97 %) was purchased from MERCK (Sigma Aldrich, Israel). Alumina N - Super I was purchased from MP Biomedicals (Enco, Israel).

2.2. Methods

2.2.1. Accelerated oxidation stability experiment

To assess the effect of oil MCs on oil oxidation kinetics, the oil was initially stripped of any polar molecules based on a modified stripping procedure applied elsewhere (Hoppenreijs et al., 2021). The canola oil was stirred overnight with alumina powder (1:1, v/v) in a 50 ml polypropylene centrifuge tube on a head-over-tail rotator. Consequently, the alumina powder with the absorbed polar molecules was removed by applying two centrifugation cycles at 500 g for 10 min. The resulting oil was completely transparent and stored capped at 253 K until further use.

Four systems were prepared, containing SO, SA, GMS, and pure stripped canola oil as a control system. For the systems containing the MCs, the stripped oil was mixed with the compounds on a hot plate to achieve a final concentration of 5.56 mmol of MC per kilogram of oil. All systems were covered with aluminum foil and heated on a magnetic stirrer hotplate until reaching 348 K to ensure complete dissolution of the MCs while minimizing light exposure. The concentration of 5.56 mmol per kilogram of oil was chosen based on the highest concentration at which GMS was remained completely dissolved after cooling, and is within the typical range of the FFA content (Chen et al., 2011a). The control stripped canola oil system was treated with the same heating procedure without adding MCs.

The thermal oxidation experiment was carried out in 10 ml glass vials containing 2 ml of a specific system. The systems were incubated at 313 K for 673 h in a dark incubator and were sampled by withdrawing the whole vials. The photo oxidation experiment was carried out in 100 ml glass beakers containing 40 g of the sample. The systems were placed under 7 LED white light lamps for 1606 h, resulting in approximately 15,000 lux illuminances. For both experiments, the vessels were covered to avoid contamination but not hermetically sealed to allow gas transfer. For the viscosity measurements, 2 ml samples were taken, while for the peroxide value (PV) and GC analysis, 100 μl samples were used. All collected samples were stored at 253 K until further analysis. The accelerated oxidation experiments were conducted in at least duplicates.

2.2.2. Peroxide value

The primary oxidation products' concentration was monitored by measuring the systems' peroxide value (PV) using the modified

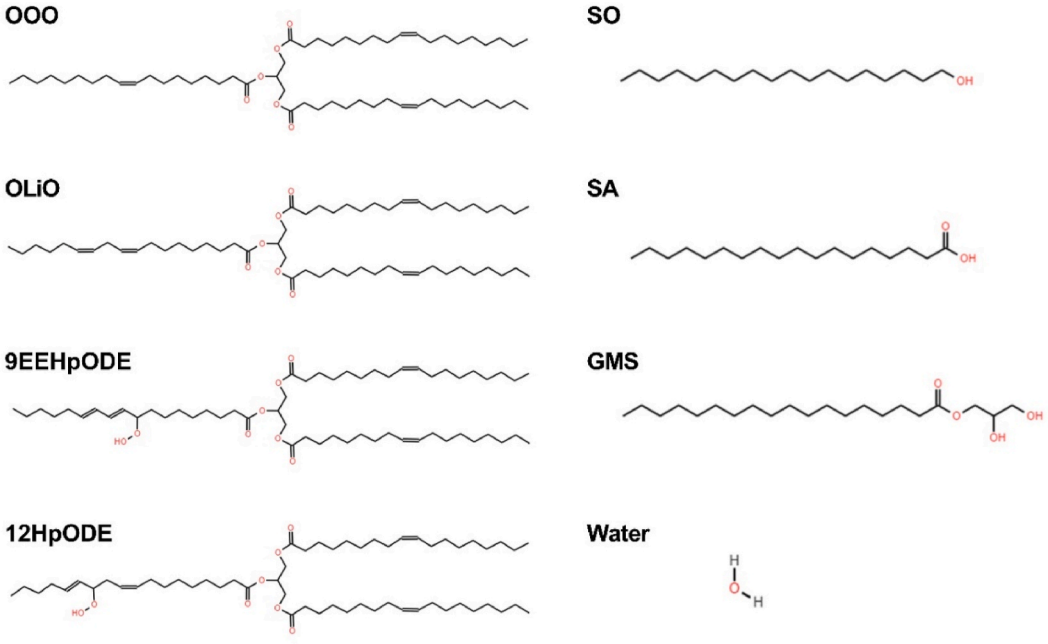

Fig. 1. The chemical structure of the studied molecules.

International Dairy Federation (IDF) 74:2006 ISO 3976:2006 method (Mehta et al., 2015; Hwang et al., 2018). First, 30 μl of the oil sample was weighed and diluted in 4.97 mL of a 7:3 (v/v) chloroform/methanol solution. This solution was further diluted by transferring 50 μl to a new test tube and adding 9.85 mL of the chloroform/methanol solution. Then, 50 μl of an ammonium thiocyanate solution and 50 μl of an iron (II) solution were added, and the samples were vortexed and allowed to stand for 5 min. Finally, the absorption at a wavelength of 500 nm was measured using a Thermo Scientific Genesys 50 spectrophotometer, and the readings were compared with a calibration curve (Fig. S1). For every reading, a blank was subtracted, which was prepared using the same procedure but in the absence of oil.

2.2.3. Viscosity

The sample viscosity was measured using an MCR 302 rheometer (Anton Paar, Prime Lab Scientific, Israel) with sandblasted parallel plates (25 mm diameter) and a 1 mm gap. The thermally oxidized systems were measured at 313 K, and the photo oxidized systems at 298 K (room temperature), corresponding to the temperature at which their accelerated oxidation experiments were conducted. For every measurement, 500 μl of the sample was used, and a shear rate ranging from 0.1 to 100 s^{-1} in a logarithmic ramp was utilized. Acknowledging the well-established Newtonian fluid behavior of oil (Diamante and Lan, 2014) and neglecting the noise at low shear rates, the average viscosity was used to build the viscosity plot as a function of oxidation time. A typical viscosity versus shear rate plot is presented in Fig. S2, where the horizontal line represents the fitted average.

2.2.4. Fatty acid content

The fatty acids (FAs) composition throughout the oxidation process was determined by gas chromatography with flame ionization detection (GC-FID). First, the oil triacylglycerols were converted to fatty acid methyl esters (FAMEs). Approximately 50 mg of the oil sample was dissolved in 10 ml of n-hexane, and 100 μl of 2N KOH in a methanol solution was added. The solution was vortex-mixed for 30 s to ensure thorough mixing of the reagents and centrifuged at 6000 rpm for 1 min (Hwang et al., 2018). After centrifugation, 2 ml of the supernatant was transferred to the GC autosampler vial. The GC separation and detection program followed the procedure introduced by Pehlivanoglu et al. (2018). The GC-FID instrument used was the 6890N, equipped with a capillary DB-23 column (60 m by 50 μm by 0.25 μm, Agilent Technologies, CA, USA) and a flame ionization detector.

Peak identification was done by comparing the GC peaks with a commercial FAME standard (data not shown). Peak quantification was performed by analyzing the chromatograms using the GaussMod model developed by OriginPro 8.5 (OriginLab Corporation, USA) for chromatographic peaks deconvolution. A typical chromatogram and peaks deconvolution are presented in Fig. S3. Palmitic acid (PA) was used as an internal standard due to its saturation and complete separation from other peaks. Consequently, the unsaturated fatty acids (USFAs) content was expressed as the ratio between the USFAs peak area and the PA peak area. All GC-FID measurements were conducted in duplicate.

2.2.5. Molecular dynamics simulation

The molecular self-assembly and interactions between the MCs, LOOHs and water molecules, were studied using MD simulations. A canola oil model, constructed of 1260, 700, and 100 molecules of OOO, OLiO, and water, respectively, was used. This model was based on the typical canola oil molar ratio (Kittipongpittaya et al., 2016; Neff et al., 1994). Additionally, 140 molecules of either 9EEHpODE or 12HpDOE were introduced to model LOOHs formed during photo or thermal oxidation, respectively. The LOOHs were added at the expense of OLiO, assuming that LiA is oxidized much faster than OA due to its higher number of double bonds (Kato et al., 2018). Finally, in the systems containing the MCs, 20 of these molecules were added at the expense of both OLiO and OOO. A total of eight simulation boxes were prepared, with the total number of molecules in each simulation box presented in Table S1, and the molecules used chemical structure shown in Fig. 1.

The initial molecular configuration was prepared with a random distribution of molecules in a cubic box using PACKMOL software (Allouche, 2012), and the simulations were conducted using GROMACS 2018.2 (Abraham et al., 2015). Prior to the production runs, the simulation box was equilibrated following the procedure outlined in our previous studies (Golodnizky et al., 2022, 2023). In brief, a series of simulations at 408 K were performed, where the pressure (p) was changed as follows: (i) $p = 1$ bar for 0.6 ns; (ii) $p = 100$ bar for 0.5 ns; and (iii) five consecutive simulation runs at $p = 1$ bar for 1 ns. Following this procedure, a constant liquid density was achieved during the last run. Temperature and pressure were controlled using a Nosé-Hoover thermostat ($\tau = 5$ ps) and a Parrinello-Rahman barostat ($\tau = 20$ ps; compressibility of 4.5×10^{-5} bar^{-1}), respectively. A timestep of 2 fs was used in all simulations.

The photo oxidation system was simulated at 298 K and the thermal oxidation system at 313 K, corresponding to the temperatures used for the accelerated oxidation stability experiments. To ensure the system's equilibrium at the target temperatures, an additional equilibration simulation of 40 ns was conducted before the production runs. To accurately assess the interaction tendencies of the molecules and mitigate any random molecular proximity effects, following the production simulation, at least four additional simulations were carried out as follows: (i) 10 ns at 408 K, (ii) equilibration for 10 ns at the target temperature, and (iii) another production for 10 ns at the target temperature. This procedure allowed the molecules to disassociate from any formed bonds during the 408 K simulation and rearrange during additional equilibration and production simulations.

In the current research, the force field parameters used were similar to those we previously tested and validated, but with several additions (Golodnizky et al., 2022): (i) the "Long-Optimized Potentials for Liquid Simulations" (L-OPLS) force field (Moultos et al., 2016) was used to model the alkyl chains; (ii) the "Optimized Potentials for Liquid Simulations – All Atoms" (OPLS-AA) (Jorgensen et al., 1996) to parametrize the central glycerol group, the polar head groups of GMS, SA, and SO, and the double bonds of the alkyl chain of OA; (iii) the extended simple point charge (SPC/E) model was used to model the water molecules (Berendsen et al., 1987); and (iv) the peroxide groups attached to the alkyl chains were parametrized based on an ab initio calculation done in our previous publication (Golodnizky et al., 2025).

The final full force field used in the current research can be seen in Tables S1–S5. All simulation input files were prepared using the DLPGEN program (Bernardes, 2022). All 3D images were prepared using the visualization software visual molecular dynamics 1.9.3 (VMD) (Humphrey et al., 1996). The simulation output xtc files, which contain the coordinates of the atoms in the simulation box were used for the calculation of the radial distribution function (RDF) using the STRFACT program (Bernardes et al., 2018; Bernardes, 2021).

3. Results and discussion

3.1. Oxidation kinetics

The stripped oil, with and without added MCs, was oxidized under a powerful light source at room temperature or in a dark incubator at 313 K. This experimental design allowed to explore the effect of surface-active molecules on the formation and organization of LOOHs under different storage conditions. The complete oxidation kinetics for both systems clearly demonstrate the well-established three oxidation regions: lag, exponential, and termination (Fig. 2 A and B for thermal and photo oxidation, respectively).

In the current research, the duration of the lag region was determined by calculating the intersection between a horizontal line fitted to the initial, almost constant PV region, and the line with positive slope fitted to the exponential period (Fig. 2 C and D for thermal and photo

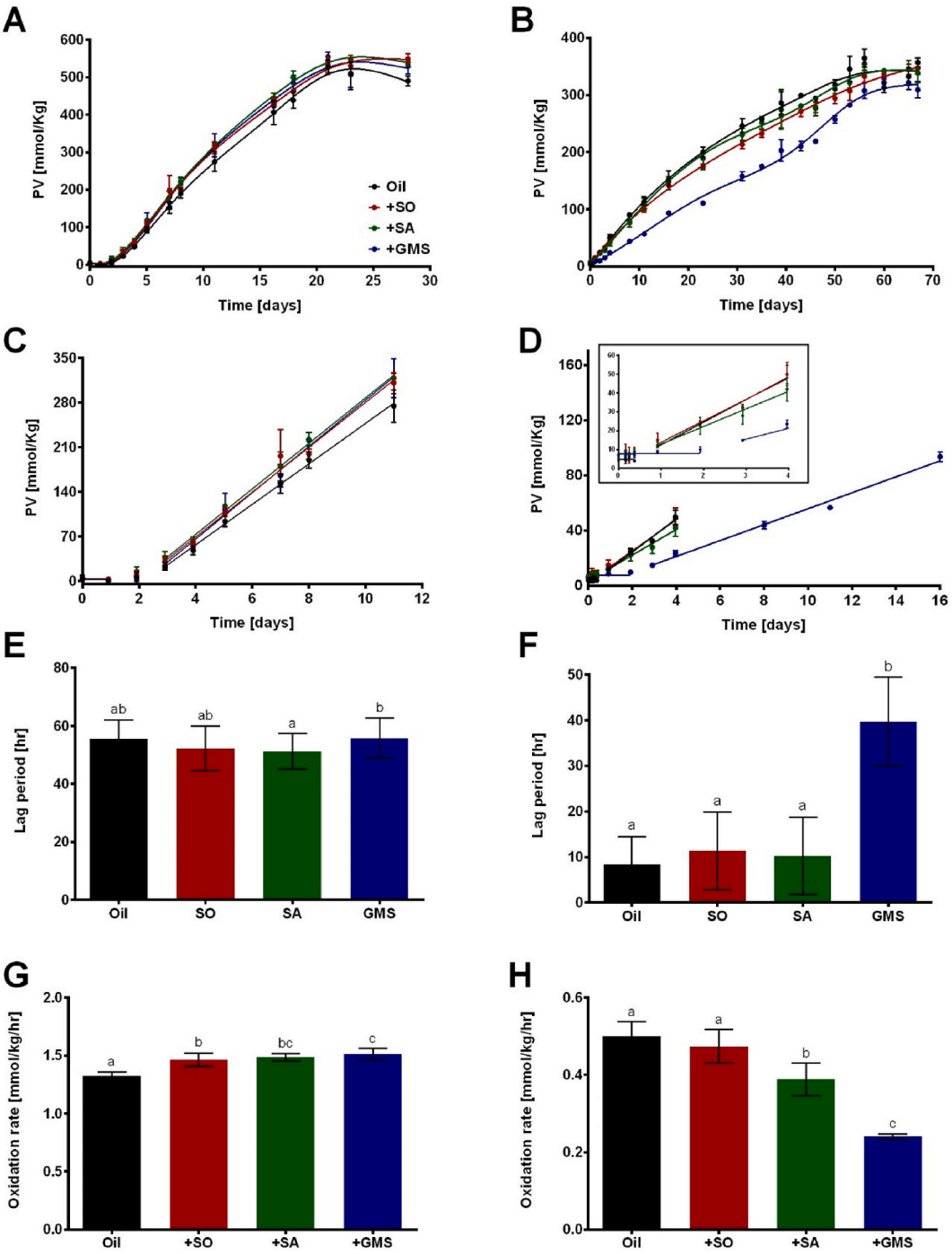

Fig. 2. The PV as a function of oxidation time as measured for the thermal (A) and photo (B) oxidation systems. The connective lines represent the spline fitting of the points to emphasize the PV changes over time. The initial PV values and the fitted linear regression lines for the thermal (C) and photo (D) oxidation systems. The lag period times as calculated for the thermal (E) and photo (F) oxidation systems using the intersections of the fitted linear lines in (C) and (D). The initial slopes fitted for the exponential period, indicating the initial oxidation rate for the thermal (G) and photo (H) oxidation systems.

oxidation, respectively), based on a common method used by others (Farhoosh, 2018; Zlatkevich, 2002). Using this method, the lag period calculated for all systems showed a value of about 60 h in the thermal oxidation experiments (Fig. 2 E). This observation suggests that the added MCs did not affect the thermal oxidation stability of the stripped canola oil at the MCs concentration and temperature used in the current experiment, in agreement with previous studies (Delfanian et al., 2023). However, in the photo oxidation experiment, the addition of GMS significantly prolonged the lag period from about 10 h, which is the value found for the other samples, to about 40 h (Fig. 2 F), suggesting that even at such a low concentration, GMS protects the stripped oil from photo oxidation and delays the period at which the formation of LOOHs accelerates. The antioxidant activity of monoglycerides such as GMS was also suggested before (Gomes et al., 2010).

Most MCs are polar molecules that, in addition to their ability to self-assemble at the water-oil interface, are also capable of forming molecular structures in bulk oil (Chen et al., 2011a; Kittipongpittaya et al., 2016). The ability of GMS to protect stripped canola oil from photo oxidation can be attributed to the ability of MAGs to self-assemble and form lamellar structures in bulk oil at room temperature (Earnden et al.,

2022; Sagalowicz et al., 2006). In our previous study, we showed that among the different MCs used in the current work, GMS possesses the highest ability to self-assemble in bulk oil. It was demonstrated that at low MC concentrations, such as those used in the current research, the dominant forces driving molecular self-assembly in bulk oil are hydrogen bonds, which GMS is more capable of forming due to its larger polar head group (Golodnizky et al., 2021). These structures in the bulk oil can scatter light from the light source, leading to mild turbidity in the GMS-containing samples. This scattering reduces the amount of light absorbed by the sample, thus reducing the energy absorption responsible for initiating the oxidation reactions (Biswas et al., 1999). We hypothesize that this higher self-assembly ability enabled the added GMS molecules to form molecular structures in the bulk stripped oil at room temperature which can scatter the light and reduce the energy absorbed by the oil, thus prolonging the lag period. Based on this theory, the results shown in Fig. 2, and the smaller polar groups of SO and SA, we suggest that the self-assembly tendency of these surface-active molecules is lower, thus their presence less affects the lag period. In the thermal oxidation experiment, due to the higher temperature and the dependency of the self-assembly process on temperature (Mata et al., 2005; Chauhan et al., 2014), it is reasonable to assume that such structures were less formed at the beginning of the thermal oxidation experiment. Therefore, the absence of these structures hinders their antioxidant activity, thus not affecting the lag period. It is worth noting that an attempt to characterize these molecular structures was conducted using X-ray diffraction and differential scanning calorimetry, but probably due to the low concentration of the added MCs, no signal was recorded (data not shown), however, a mild sample turbidity could be clearly seen. In further research, other methods, such as Cryogenic electron microscopy or light scattering techniques might provide more conclusive evidence for such structures, however, these methods were out of the scope of the current study.

After the lag period, the PV increases and the LOOHs accumulate in the oil, indicating the beginning of the second period, the exponential period. At this point, the LOOHs accumulation rate can be ascribed to the oxidation rate (Hoppenreijs et al., 2021; Choe and Min, 2006). To obtain a proper statistical analysis, the accelerated shelf-life experiments replicates were all plotted in the same plot, and the regression fitting parameters and their standard deviations were calculated. The initial increase in the PV curves was fitted by a linear regression line (Fig. 2 C and D, for the thermal and photo experiments, respectively) and the slopes can represent the oxidation rates (Fig. 2 G and H, for the thermal and photo experiments, respectively). In the thermal oxidation experiment, the addition of the MCs slightly increased the initial oxidation rate, suggesting a mild pro-oxidant activity. Such an acceleration of the thermal oxidation rate in the presence of different MCs, such as SO, glycerol-monopalmitate, tetradecanol, and different antioxidants was previously shown by others (Chaiyasit et al., 2007b; Kortenska et al., 2002). Interestingly, in the photo oxidation experiment, the opposite effect was observed, where the addition of MCs decreased the initial oxidation rate, suggesting an antioxidant activity. These opposed trends can be ascribed to the ability of the MCs and LOOHs molecular organizations to scatter light, as was suggested earlier and will be further discussed in the next chapters.

The third region, termed the termination period, is characterized by a relatively constant or even reducing PV, resulting from an equal or higher LOOH decomposition compared to their formation rate (Brodnitz, 1968; Hoppenreijs et al., 2021; Merkx et al., 2018). Such a change in the rates ratio is ascribed to the dramatic decrease in the polyunsaturated FAs (PUFAs) content which is the substrate for the oxidation reaction. The termination stage was achieved after approximately 500 h in the thermal oxidation experiment for all the systems (Fig. 2 A). This observation suggests that the addition of the MCs did not affect the balance between the LOOH formation and decomposition rates in the thermal oxidation experiment. In the photo oxidation experiment, this stage was not clearly achieved for most of the systems in the time frame of the current study, even after more than 1600 h (Fig. 2 B). In general, at such a high oxidation degree, there are various secondary oxidation products that also affect the oxidation kinetics; thus, in this region, the effect of the added MCs alone is hard to determine and is expected to be reduced (Jo and Lee, 2021).

The total oxidation process was also monitored by measuring the FA content over the oxidation experiments. In contrast to the PV curves, measuring the FA content allows the assessment of the total consumption rate of the USFAs by the oxidation reaction. This measurement enables us to monitor not only the formation of the primary oxidation products but also the secondary products. The total USFA content was monitored over the oxidation process and normalized using the PA content as an internal standard. For the thermal oxidation processes, all systems exhibited similar behavior (Fig. 3 A). Moreover, even in the termination region, as emphasized in the PV curves, at oxidation times above 500 h, the USFA consumption continued. This observation agrees with our suggestion that, during this period, the oxidation process did not terminate, but the LOOH decomposition rate equalized or surpassed their formation rate.

For the photo oxidation processes, the system containing GMS clearly exhibited higher USFA content throughout the oxidation process (Fig. 3 B). This observation can be attributed to the lower oxidation rate calculated from the PV curve for the GMS-containing striped oil (Fig. 2 H). At the beginning of the oxidation exponential period, when a low amount of the USFAs was consumed by oxidation reactions, such rate differences were not emphasized. However, at more advanced oxidation stages, higher amounts of USFAs were consumed by the oxidation reaction, thus these oxidation rate differences became detectable in the FA content measurement. Therefore, noticeable differences in USFA were observed in the GMS compared with the other MCs.

The total GC chromatograms were deconvoluted to monitor the changes in specific FA content (Fig. S4). In both experiments, the decrease in the OA content was the lowest (Fig. S4 A and B), while the decrease in the LnA content was the highest (Fig. S4 E and F). Such a trend can be related to the lower energy required for hydrogen dissociation between two double bonds, as found in LiA and LnA, compared to only one, as found in OA (Schaich, 2020; Kerrihard et al., 2015).

3.2. Molecular self-assemblies

The LOOHs concentration gradually increases after the lag period and during the exponential period. Due to their amphiphilic nature, LOOHs can self-assemble and form different molecular self-assemblies (Ghnimi et al., 2017). These self-assemblies have been shown to increase the oxidation rate and change the kinetic order of the oxidation reactions (Farhoosh, 2018; Nguyen et al., 2024; Brimberg, 1993; Chaiyasit et al., 2008). Moreover, these molecular self-assemblies are marked by sharp changes in the physical properties of the oil, such as surface tension, conductivity, turbidity, nuclear magnetic resonance spectra, and viscosity (Priyanto et al., 2001).

Flow behavior measurement is a popular tool used for structural analysis in various fields, such as emulsifiers, organic molecules, and computational chemistry (Priyanto et al., 2001; Alasiri, 2019; Wu et al., 2014; Kamranfar and Jamialahmadi, 2014). In the current research, the molecular self-assembly in striped canola oil with and without the oil MCs was characterized over the oxidation process by monitoring the oil viscosity. At the beginning of the oxidation experiment, when the LOOH concentration is relatively low, they are expected to be homogeneously dispersed in the bulk oil, thus not significantly resisting the applied shear forces. Therefore, a Newtonian behavior with no significant change in viscosity compared to unoxidized oil is expected. Above the LOOH CMC, LOOHs are expected to self-assemble and form reverse micelles. These reverse micelles increase the resistance to the applied shear force during flow in viscosity measurement, leading to an increased measured viscosity. Such a transition from an approximately constant viscosity at the beginning of the oxidation process to an

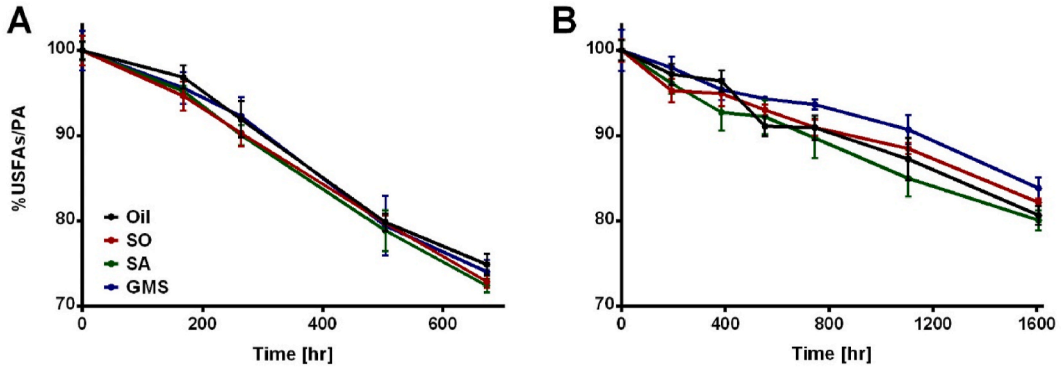

Fig. 3. The ratio of the total USFA:PA as a function of oxidation time, as was measured for the thermal (A) and photo oxidation systems (B).

increasing viscosity over time can be seen in Fig. 4 A and D for the thermal and photo oxidation experiments, respectively. As the LOOH concentration increases with the progress of oxidation, these micelles size increases and new micelles are formed, further increasing the oil viscosity. This growth and formation of reverse micelles will continue until interactions between the micelles occur and a continuous meso-phase is formed. Such mesophase formation will lead to a significant increase in the measured viscosity (Ghnimi et al., 2017; Brimberg and Kamal-Eldin, 2003). It is worth noting that viscosity measurements provide an indirect indication of the formation of such molecular structures. However, within the scope of the current study, we propose that this indirect indication is sufficient to enable a reliable comparison of the effects of the different minor components' polar groups. Additionally, it is important to mention that polymerization reactions may occur during storage. However, these reactions become dominant primarily at high temperatures, such as during frying, and in low-oxygen environments, and are therefore not expected to be significant under the current experimental conditions. (Dobarganes and Márquez-Ruiz, 2007; Velasco and Dobarganes, 2002).

The change in the rate at which the viscosity increases can be seen in Fig. 4 A and D for thermal and photo oxidation, respectively. The intersections between the different regions in the viscosity curves were used to calculate the time at which the reverse micelles and meso-phase were formed for each system (Fig. S5). These times were then translated to LOOH concentrations, expressed by the PV, using a linear regression of the PV plots (Fig. S6). In the thermal oxidation experiment, the addition of SA to the striped canola oil resulted in a significantly lower LOOH concentration at the reverse micelles formation, while the addition of SO and GMS showed no significant effect (Fig. 4 B). In the photo oxidation experiment, all added MCs decreased the LOOH CMC, with GMS having the highest effect (Fig. 4 E). The effect of different surface-active molecules on the LOOH CMC has been previously discussed by others. It was shown that LOOHs can be incorporated into the reverse micelles formed by other surface-active molecules, leading to a decrease in the LOOH concentration required to reach the CMC (Chen et al., 2011a). For example, in the presence of polyglycerol polyricinoleate (PGPR) and/or curcumin, the LOOH CMC was decreased, suggesting that PGPR, curcumin, and LOOHs can stabilize the water/oil interface together and form mutual reverse micelles (Jokar et al., 2022). Based on the results shown in Fig. 4 B and E, it seems that SA was able to form mutual reverse micelles with LOOHs, thus decreasing the critical concentration of LOOHs required to stabilize the water/oil interface and form these micelles. This hypothesis is also supported by the findings of Chaiyasit et al. (2007b), who showed that the addition of OA to oil decreased the reverse micelles' size formed by the LOOHs. Such a decrease in micelle size leads to a larger water/oil interface, implying that the addition of OA to oxidized oil, combined with the LOOHs, had a synergistic effect on interface stabilization. It is worth noting that

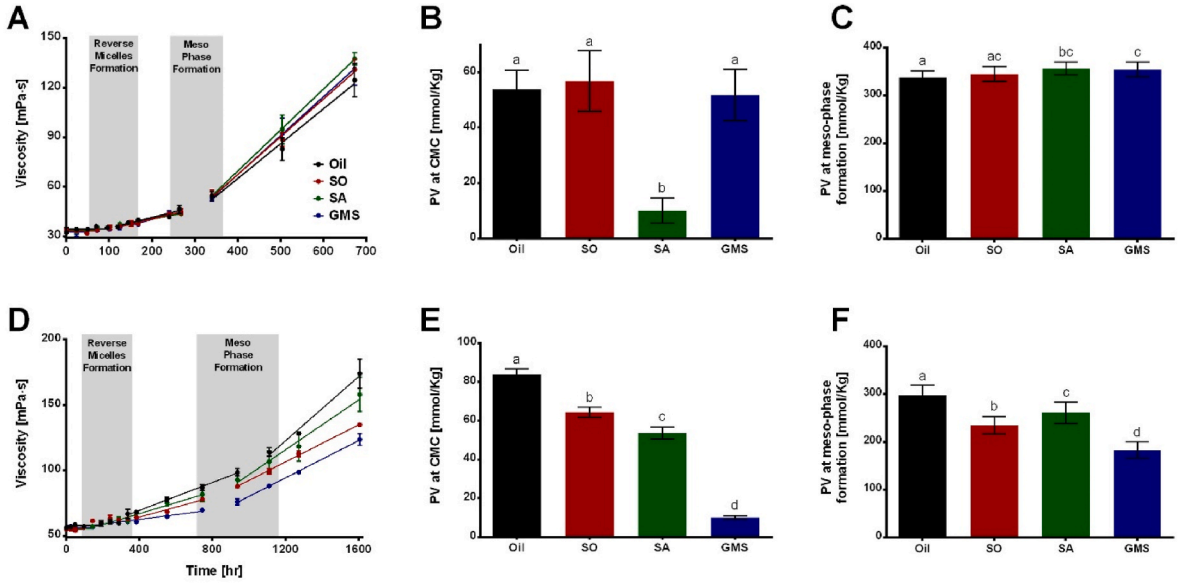

Fig. 4. Viscosity values as a function of oxidation time for the thermal oxidation (A) and photo oxidation (D) systems. Linear regression lines are included in the plots, representing the calculations used for determining the micelle formation times. These times were used to calculate the PV at the CMC and the meso-phase formation time for the thermal (B and C) and photo (E and F) oxidation systems, respectively.

deviation in the region definition may slightly affect the calculated cross-section values, thereby increasing the uncertainty in the absolute values obtained in this study. However, since the primary focus is the comparison between the effects of the different minor components' polar groups on molecular organization, such variations did not impact the overall trends or conclusions. Interestingly, the addition of GMS did not affect the thermal LOOH CMC while significantly decreasing it in the photo oxidation experiment. This observation strengthens our assumption that GMS form a unique organization in bulk oil, at the beginning of the photo oxidation experiment at room temperature, probably into lamellar structures (Earnden et al., 2022; Sagalowicz et al., 2006). Such structures seem to be less presented at the high temperature in the thermal oxidation experiment. It appears that in the photo oxidation experiment, GMS was able to form these structures from the beginning of the experiment (Fig. S5), leading to a very low LOOH concentration at the reverse micelles' formation time (Fig. 4 E). Such a decrease in the time required to reach CMC (Fig. S5 C) and the concentration at this point (Fig. 4 E) seemed to produce an antioxidant effect on the oil oxidation rate rather than a pro-oxidant effect (Fig. 2 F and H), as could be expected based on previously proposed oxidation kinetic theories (Brimberg, 1993).

The effect of MAGs on the thermal oxidation process was also examined by Delfanian et al. (2023), who showed that in combination with other surface-active molecules, MAGs can decrease the thermal oxidation LOOH CMC. The results presented here suggest that in the photo oxidation process, GMS can promote reverse micelle formation and retard the photo oxidation process without the addition of other amphiphilic molecules. Interestingly, Delfanian et al. (2023) showed that such an effect on the LOOH CMC did not affect the lag period, which is directly related to oil oxidation stability. The absence of an effect on the lag period suggests that changes in the CMC do not necessarily affect oil stability. Such effect of LOOH CMC on oil stability agrees with our findings in the thermal oxidation experiment, while in the photo oxidation experiment, we showed that the CMC change results in an antioxidant effect, hence longer lag period and better oxidation stability.

Considering the effect of SO and SA, lower LOOH CMC were observed in the presence of these molecules during the photo oxidation experiment (Fig. 4 E) and in the presence of SA in the thermal oxidation experiment (Fig. 4 B), compared with the oil samples. Such lower LOOH CMCs did not affect oil oxidation stability, as expressed by the similar lag period as the oil system (Fig. 2 E and F). Interestingly, even though the addition of SA decreased the LOOH CMC in both experiments, it increased the initial oxidation rate in the thermal oxidation experiment, while it decreased it in the photo oxidation experiment. This observation can be explained by the different energy sources used in these experimental designs. It has been previously shown that the addition of free FAs decreases the pH of the water droplets inside the formed reverse micelles during the oxidation process (Kittipongpittaya et al., 2014). Such a pH reduction promotes oil oxidation by accelerating reactions catalyzed by acids, thus increasing the oxidation rate (Kittipongpittaya et al., 2014, 2016). On the other hand, in the photo oxidation experiment, molecular structures in bulk oil scatter the light, thus reducing the energy absorbed by the PUFAs in the oil and decreasing the oxidation rate (Biswas et al., 1999). In the photo oxidation experiments, it seems like the lower energy absorption had a higher impact compared to the reaction acceleration by acidic catalysis mentioned above, while in the thermal oxidation experiment, such structures, even if existed in a very low amounts, did not affect heat energy absorption.

A continuous meso-phase is formed when the reverse micelles occupy a large volume of the bulk oil and start to interact with each other. The interaction tendency of these micelles is strongly dependent on their interface molecular composition, where the MCs and oxidation products are accumulating (Wang et al., 2024; Chaiyasit et al., 2007b; Delfanian et al., 2023). In the current research, such continuous meso-phases were formed in an advanced oxidation stage, at PVs above 200 mmol/kg oil for both experimental conditions (Fig. 4 C and F), when a significant amount of USFAs was already consumed by the oxidation reaction (Fig. 3). At such an advanced oxidation stage, the secondary oxidation products' concentration is expected to be very high, adding various additional surface-active molecules to the bulk oil. In the study of Jo and Lee (2021), it was shown that secondary oxidation products such as hexanal, propanal, and nonanal can affect the reverse micelles formation, thus probably affecting micelle-micelle interactions and meso-phase formation. Based on the results in the current research, the LOOHs concentration required for such meso-phase formation was increased by the addition of MCs in the thermal oxidation experiment, while it was decreased in the photo oxidation experiment. Such differences may be attributed to the total polar molecular concentration, and further sophisticated analysis of the chemical composition at this stage, is required. Considering the high PVs, at this stage, the oil contains a very high amount of toxic and unpleasant compounds, making it dangerous for human consumption; therefore, this issue was out of the scope of this research and no further analysis was conducted.

3.3. Molecular dynamics simulation perspective on interaction tendencies

The molecular composition of the water/oil interface plays a crucial role in the molecular organization of LOOHs and the oxidation kinetics (Wang et al., 2024). Molecular dynamics simulation is a widely used tool for evaluating the molecular composition of the water/oil interface (Smith, 2022; Chen et al., 2021; Siani et al., 2016; Agmon et al., 2018). Due to the short time and length scales of all-atom MD simulations, the formation of water droplets and water/oil interfaces cannot be achieved in these simulations (Packwood et al., 2017). Therefore, in the current research, the tendencies of the oil MCs to interact with water and other LOOHs were examined. These tendencies were then interpreted and projected onto the self-assembly potency of the different molecules during the oxidation process. In the MD simulations, the thermal and photo oxidation systems were distinguished by the type of LOOHs in the simulation boxes, with 9EEHpODE and 12HpODE (Fig. 1) used for the thermal and photo oxidation simulations, respectively.

Radial distribution function (RDF) is a widely used tool to study the interactions of different molecules (Moradi et al., 2019). This tool calculates the probability of finding different moieties at specific distances. Such distances can then be related to different interactions and molecular bonds, providing valuable information about the organization and aggregation tendencies of the molecules. Here, RDFs were calculated considering the water and the different surface-active molecules to assess their tendency to interact with each other. Unsurprisingly, the RDFs calculated for the distances between the water molecules show the sharpest and most intense peak centered at about 2.8 Å (Fig. 5), which is the characteristic distance between water oxygens involved in hydrogen bonds (Moradi et al., 2019). This peak showed exceptionally high intensity values above 600 in both simulations, suggesting that the tendency of the water molecules to form hydrogen bonds between themselves is extremely high (Fig. 6). Such tendency is expected due to the high hydrophobic environment the water molecules experience in the oil phase, thus driving their bonding and aggregate formation.

The tendency of surface-active molecules to organize in reverse micelles can be discussed in terms of their ability to form hydrogen bonds with water. In lipid solutions such as edible oils, van der Waals interactions can be formed between the oil TAGs and the hydrophobic regions of the amphiphilic molecules. Therefore, the role of these interactions in reverse micelle formation is reduced, positioning polar interactions, specifically hydrogen bonds, as the main driving force (Qiao et al., 2014). In the current systems, hydrogen bonds can be formed between the water, MCs, and LOOHs molecules. To evaluate the tendency of these hydrogen bonds to form, RDFs were calculated considering the distances between water and LOOH molecules, water and MCs molecules, and MCs and LOOH molecules (Fig. 5). The maximum intensities of the peaks corresponding to hydrogen bonds were extracted from the RDF curves (Fig. 6), which can be ascribed to

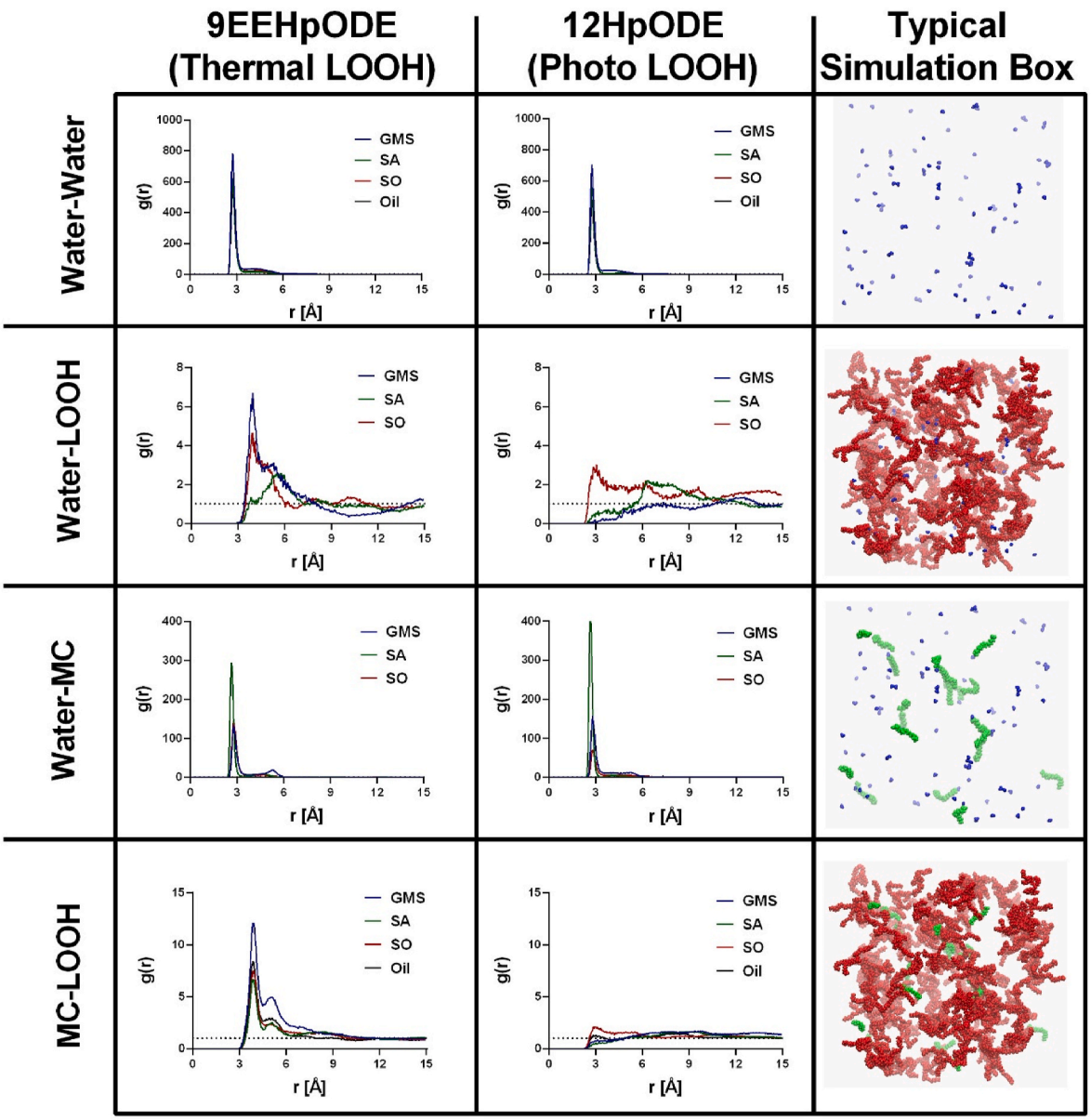

Fig. 5. Typical RDFs computed between the different molecules for thermal and photo oxidation simulations. In the typical simulation box, the molecules were colored by their type: water molecules - blue, LOOHs - red, and MCs -green. For a clear presentation, only the simulation box of the system containing SA is presented.

the tendency of a specific hydrogen bond to be formed.

The results shown in Figs. 5 and 6 suggest that the tendency of MCs and water molecules to form hydrogen bonds is higher than their tendency to form these bonds with LOOHs or the tendency of LOOHs to form hydrogen bonds with water. This observation can be expected due to the more exposed polar group of the MCs compared to the peroxide group of the LOOHs, which is located on the fatty acid chain and is under high steric interference. Moreover, the tendency of SA to form hydrogen bonds with water was the highest in both photo and thermal oxidation, as indicated by the higher RDF peak maximum intensity (Fig. 6). This high tendency suggests that SA tends to bind water more than GMS and SO, thus possessing higher surface activity. This higher surface activity might lead to the lower CMC observed in the experimental results, where, in addition to the SA molecules, fewer LOOH molecules were required to form stable reverse micelles (Fig. 4 B and E). Interestingly, in the photo oxidation experiment, the addition of GMS to the stripped oil resulted in the lowest CMC (Fig. 4 E), even though the tendency of GMS to form hydrogen bonds with water was lower than that of SA. This observation can be explained by the higher tendency of GMS to form its own structures, as discussed in section 3.2 and in our previous work (Golodnizky et al., 2021). Such a molecular self-assembly of GMS might be the reason for the early intersection between the first two regions in the viscosity curves (Fig. 4 D) and resulting in a very low LOOH CMC (Fig. 4 E). In the thermal oxidation experiment, such molecular self-assemblies of GMS were not formed due to the higher temperature, thus the recorded CMC was higher and not significantly different from the one recorded for the control stripped oil, in agreement with the hydrogen bonding tendency shown in Fig. 6 for the thermal oxidation model containing GMS. Considering the effect of SO addition, it showed a lower tendency to form hydrogen bonds with water than SA, leading to a higher CMC under both experimental conditions (Fig. 4 B and E). Compared with GMS, SO exhibited an equal tendency to form hydrogen bonds with water, suggesting similar surface activity in the examined systems. Such similar surface activity and the lower ability to self-assemble in bulk oil during the photo oxidation experiment resulted in higher (Fig. 4 E) and similar (Fig. 4 B) CMC compared with the GMS containing system in the photo and thermal oxidation experiments, respectively.

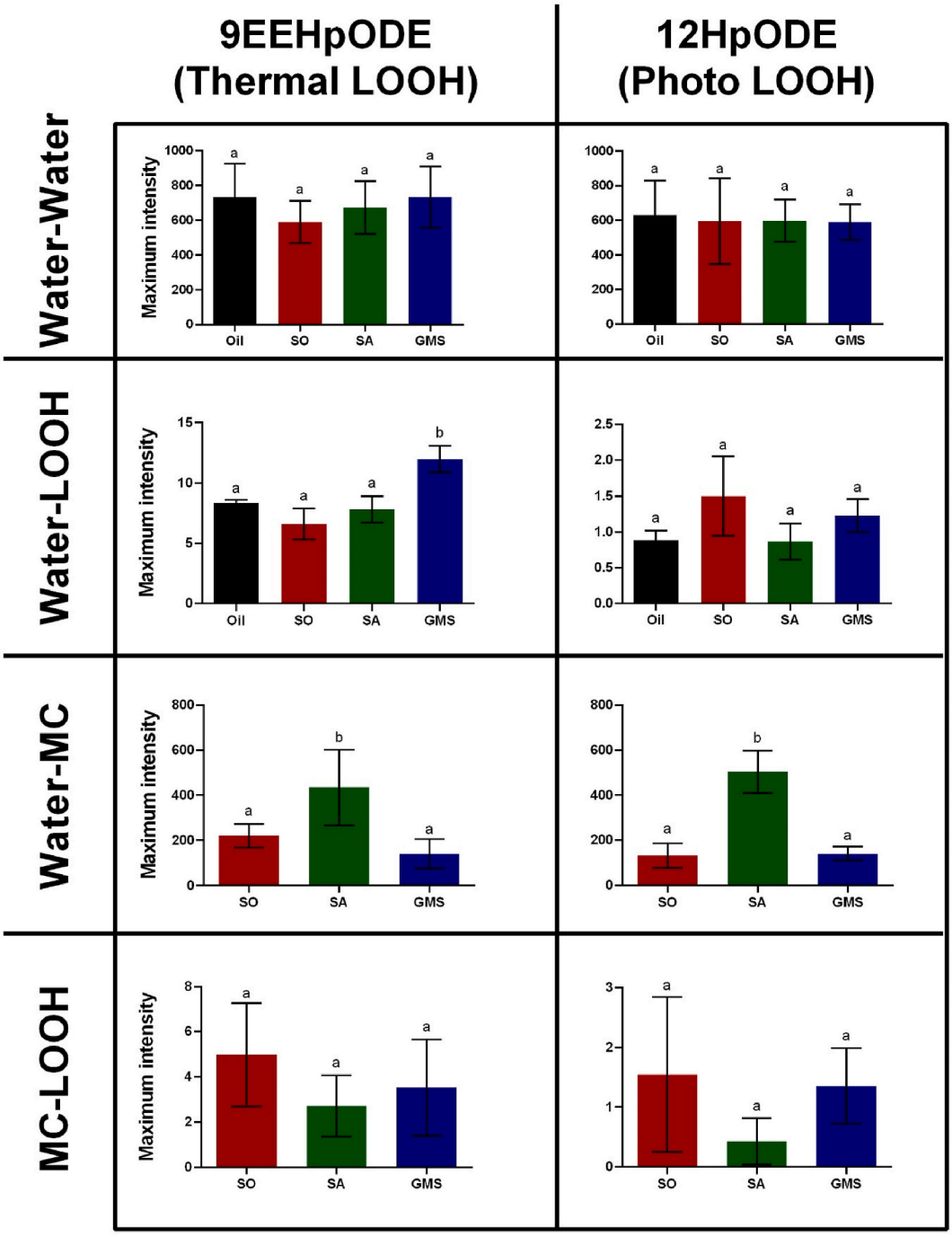

Fig. 6. The maximum intensities of the RDF peak correspond to the hydrogen bonds formation between the water, different MCs, and different LOOHs, as was calculated for the thermal and photo oxidation simulations.

The addition of MCs to the model does not seem to affect the tendency of LOOHs to form hydrogen bonds with water or with the MCs in most systems, even though experimentally we showed that it affected the CMC. Based on this observation, we hypothesized that the lower CMCs observed in Fig. 4 result from the ability of the LOOHs to form mutual reverse micelles with the added MCs, rather than improving their ability to form these micelles by themselves at lower concentrations. This hypothesis is in agreement with previous studies that related the effect of surface-active molecules on the LOOH CMC to their ability to form mutual reverse micelles (Wang et al., 2024; Jo and Lee, 2021; Delfanian et al., 2023; Jokar et al., 2022). In these studies, it was suggested that amphiphilic molecules such as antioxidants, PGPR, phospholipids, aldehydes, and other surface-active molecules can occupy the water/oil interface alongside the LOOHs, rather than pushing the LOOHs to the bulk oil phase. It was suggested that such mutual coexistence at the interface is responsible for the decrease in the LOOH CMC observed in the presence of MCs. Moreover, while comparing the control stripped oil system, the thermal LOOHs seem to have a higher tendency to form hydrogen bonds with water compared with the photo oxidation LOOHs, leading to a lower PV at the CMC time (Black columns in Fig. 4 B and E). This phenomenon is discussed in our previous work, in which we showed that the tendency of photo oxidation LOOHs to form hydrogen bonds with water was lower, and these bonds were less stable, compared with the thermal oxidation LOOHs.

4. Conclusions

In the current research, the molecular organization of MCs and LOOHs in oil was examined with respect to oil stability under thermal and photo oxidation conditions. Four systems were studied: stripped canola oil as a control, and stripped canola oil with different added MCs such as SO, SA, and GMS. The molecular structures were assessed by viscosity measurements, the oxidation process was monitored by PV and FAs content assays, and the molecular interaction tendencies were evaluated by MD simulations. The results indicated that SO, with the smallest polar head group, showed the least influence on oil oxidation kinetics in the different experimental conditions. It did not affect the lag period and slightly increased the oxidation rate during thermal oxidation. The addition of SA significantly decreased the critical concentration required for reverse micelle formation, attributed to its high surface activity as demonstrated by the high interaction ability with water molecules in the MD simulations. SA did not affect the duration of the lag period in either experimental conditions but decreased the oxidation rate notably in the photo oxidation experiment. On the contrary, the presence of GMS in stripped canola oil significantly reduced the CMC in the photo oxidation experiment, resulting in a markedly lower oxidation rate. Moreover, it significantly improved oil oxidation stability by extending the lag period from about 10 h to about 40 h, demonstrating GMS's physical antioxidant activity in the photo oxidation experiment. However, the addition of GMS did not affect the CMC in the thermal oxidation experiment but slightly increased the oxidation rate. This difference was explained by GMS's ability to form molecular self-assemblies such as lamellae at the lower temperature found in the photo oxidation experiments, leading to early molecular organization. These assemblies seem to scatter light, thereby reducing energy absorption during photo oxidation, resulting in lower oxidation rates.

Overall, SO with the smallest polar group had the least impact on the oxidation process, while SA with its larger group exhibited the highest water-binding ability thus significantly affecting the LOOH CMC. GMS, with the largest polar group, demonstrated potent self-organization abilities that retarded photo oxidation but exhibited lower surface activity compared to SA. These findings offer a novel perspective on the role of amphiphilic molecules in oil oxidation, potentially contributing valuable insights to predict and enhance edible oil stability.

CRediT authorship contribution statement

Daniel Golodnizky: Methodology, Data curation, Validation, Formal analysis, Visualization, Writing – original draft. **Emil Eshaya:** Methodology, Data curation, Validation, Formal analysis, Visualization. **Carlos E.S. Bernardes:** Conceptualization, Methodology, Supervision, Writing – review & editing. **Maya Davidovich-Pinhas:** Conceptualization, Methodology, Supervision, Writing – review & editing.

Declaration of competing interest

The authors declare that they have no known competing financial interests or personal relationships that could have appeared to influence the work reported in this paper.

Acknowledgment

This research was supported by the Israel Science Foundation (ISF) (Grant No. 454/17), by the Technion's Russell Berrie Nanotechnology Institute (RBNI), and by Fundação para a Ciência e a Tecnologia (FCT), Portugal (projects UIDB/00100/2020: https://doi.org/10.54499/UIDB/00100/2020; UIDP/00100/2020: https://doi.org/10.54499/UIDP/00100/2020; LA/P/0056/2020: https://doi.org/10.54499/LA/P/0056/2020; and 2021.03239. CEECIND: https://doi.org/10.54499/2021.03239.CEECIND/CP1650/CT0003). We thank Inbal Rush from the laboratory of Prof. Ayelet Fishman at the Technion, Israel, for her help in the GC operation. We also thank Lorenz Plankensteiner and Vincent Boerkamp from the laboratory of Dr. Marie Hennebelle at the Wageningen university, Netherlands, for their valuable insights for the oil stripping process.

Appendix A. Supplementary data

Supplementary data to this article can be found online at https://doi.org/10.1016/j.crfs.2025.101056.

Data availability

Data will be made available on request.

References

Abraham, M.J., Murtola, T., Schulz, R., Páll, S., Smith, J.C., Hess, B., Lindah, E., 2015. Gromacs: high performance molecular simulations through multi-level parallelism from laptops to supercomputers. SoftwareX 1–2, 19–25.
Agmon, E., Solon, J., Bassereau, P., Stockwell, B.R., 2018. Modeling the effects of lipid peroxidation during ferroptosis on membrane properties. Sci. Rep. 8, 1–11.
Alasiri, H., 2019. Determining critical micelle concentrations of surfactants based on viscosity calculations from coarse-grained molecular dynamics simulations. Energy Fuels 33, 2408–2412.
Allouche, A., 2012. Software news and updates gabedit — a graphical user interface for computational chemistry softwares. J. Comput. Chem. 32, 174–182.
Berendsen, H.J.C., Grigera, J.R., Straatsma, T.P., 1987. The missing term in effective pair potentials. J. Phys. Chem. 91, 6269–6271.
Bernardes, C.E.S., 2021. STRFACT: Determining X-Ray Total Scattering Factors from Molecular Dynamics Simulation Data. https://doi.org/10.5281/ZENODO.4762008.
Bernardes, C.E.S., 2022. DLPGEN: preparing molecular dynamics simulations with support for polarizable force fields. J. Chem. Inf. Model. 62, 1471–1478.
Bernardes, C.E.S., Shimizu, K., Canongia Lopes, J.N., 2018. Comparative structural analyses in four ionic liquid systems: the two low-q peaks of IL structure factor functions. Mol. Simul. 44, 478–484.
Biswas, S., Bhattacharya, S.C., Sen, P.K., Moulik, S.P., 1999. Absorption and emission spectroscopic studies of fluorescein dye in alkanol, micellar and microemulsion media. J. Photochem. Photobiol. Chem. 123, 121–128.
Brimberg, U.I., 1993. On the kinetics of the autoxidation of fats. II. Monounsaturated substrates. J. Am. Oil Chem. Soc. 70, 1063–1067.
Brimberg, U.I., Kamal-Eldin, A., 2003. On the kinetics of the autoxidation of fats: influence of pro-oxidants, antioxidants and synergists. Eur. J. Lipid Sci. Technol. 105, 83–91.
Brodnitz, M.H., 1968. Autoxidation of saturated fatty acids. A review. J. Agric. Food Chem. 16, 994–999.
Budilarto, E.S., Kamal-Eldin, A., 2015. The Supramolecular Chemistry of Lipid Oxidation and Antioxidation in Bulk Oils.
Chaiyasit, W., Elias, R.J., McClements, D.J., Decker, E.A., 2007a. Role of physical structures in bulk oils on lipid oxidation. Crit. Rev. Food Sci. Nutr. 47, 299–317.
Chaiyasit, W., Stanley, C.B., Strey, H.H., McClements, D.J., Decker, E.A., 2007b. Impact of surface active compounds on iron catalyzed oxidation of methyl linolenate in AOT-water-hexadecane systems. Food Biophys. 2, 57–66.
Chaiyasit, W., McClements, D.J., Weiss, J., Decker, E.A., 2008. Impact of surface-active compounds on physicochemical and oxidative properties of edible oil. J. Agric. Food Chem. 56, 550–556.
Chauhan, S., Kaur, M., Kumar, K., Chauhan, M.S., 2014. Study of the effect of electrolyte and temperature on the critical micelle concentration of dodecyltrimethylammonium bromide in aqueous medium. J. Chem. Thermodyn. 78, 175–181.
Chen, B., McClements, D.J., Decker, E.A., 2011a. Minor components in food oils: a critical review of their roles on lipid oxidation chemistry in bulk oils and emulsions. Crit. Rev. Food Sci. Nutr. 51, 901–916.
Chen, B., Han, A., Laguerre, M., McClements, D.J., Decker, E.A., 2011b. Role of reverse micelles on lipid oxidation in bulk oils: impact of phospholipids on antioxidant activity of α-tocopherol and Trolox. Food Funct. 2, 302–309.
Chen, Q., Zhang, W., Mu, W., 2021. Molecular Dynamics Simulation for Food Enzyme Engineering: Why This Technique Should Be Encouraged to Learn. https://doi.org/10.1021/acs.jafc.0c07681.
Choe, E., Min, D.B., 2006. Mechanisms and factors for edible oil oxidation. Compr. Rev. Food Sci. Food Saf. 5, 169–186.
Cui, L., Kittipongpittaya, K., McClements, D.J., Decker, E.A., 2014. Impact of phosphoethanolamine reverse micelles on lipid oxidation in bulk oils. JAOCS, J Am Oil Chem Soc 91, 1931–1937.
Delfanian, M., Sahari, M.A., Barzegar, M., Ahmadi Gavlighi, H., Barba, F.J., 2023. Interfacial behavior of gallic acid and its alkyl esters in stripped soybean oil in combination with monoacylglycerol and phospholipid. Food Chem. 413, 135618.
Diamante, L.M., Lan, T., 2014. Absolute viscosities of vegetable oils at different temperatures and shear rate range of 64.5 to 4835 s − 1. J Food Process 2014, 1–6.
Dobarganes, MC, Márquez-Ruiz, G, 2007. Formation and analysis of oxidized monomeric, dimeric, and higher oligomeric triglycerides. In: *Deep Frying: Chemistry, Nutrition, and Practical Applications*, Second Edition. AOCS Press, pp. 87–110.

Earnden, L., Marangoni, A.G., Laredo, T., Stobbs, J., Pensini, E., 2022. Self-Assembled glycerol monooleate demixes miscible liquids through selective hydrogen bonding to water. J. Mol. Liq. 367, 120551.
Farhoosh, R., 2018. Reliable determination of the induction period and critical reverse micelle concentration of lipid hydroperoxides exploiting a model composed of pseudo-first and -second order reaction kinetics. Lwt 98, 406–410.
Flickinger, B.D., Matsuo, N., 2003. Nutritional characteristics of DAG oil. Lipids 38, 129–132.
Ghnimi, S., Budilarto, E., Kamal-Eldin, A., 2017. The new paradigm for lipid oxidation and insights to microencapsulation of omega-3 fatty acids. Compr. Rev. Food Sci. Food Saf. 16, 1206–1218.
Golodnizky, D., Rosen-kligvasser, J., Davidovich-pinhas, M., 2021. The role of the polar head group and aliphatic tail in the self-assembly of low molecular weight molecules in oil. Food Struct. 30, 100240.
Golodnizky, D., Shmidov, Y., Bitton, R., Bernardes, C.E.S., Davidovich-Pinhas, M., 2022. Isotropic liquid state of triacylglycerols. J. Mol. Liq. 353, 118703.
Golodnizky, D., Bernardes, C.E.S., Davidovich-pinhas, M., 2023. Isotropic liquid state of cocoa butter. Food Chem. 439, 138066.
Golodnizky, D., Eshaya, E., Bernardes, C.E.S., Davidovich-Pinhas, M., 2025. Insights into the dynamics of edible oil oxidation: from molecular interactions to oxidation kinetics. Food Hydrocoll. 164, 111203.
Gomes, T., Caponio, F., Bruno, G., Summo, C., Paradiso, V.M., 2010. Effects of monoacylglycerols on the oxidative stability of olive oil. J. Sci. Food Agric. 90, 2228–2232.
Hoppenreijs, L.J.G., Berton-Carabin, C.C., Dubbelboer, A., Hennebelle, M., 2021. Evaluation of oxygen partial pressure, temperature and stripping of antioxidants for accelerated shelf-life testing of oil blends using 1H NMR. Food Res. Int. 147, 110555.
Humphrey, W., Dalke, A., Schulten, K., 1996. Sartorius products. J. Mol. Graph. 14, 33–38.
Hwang, H.S., Fhaner, M., Winkler-Moser, J.K., Liu, S.X., 2018. Oxidation of fish oil oleogels formed by natural waxes in comparison with bulk oil. Eur. J. Lipid Sci. Technol. 120, 1–10.
Jalali-Jivan, M., Garavand, F., Jafari, S.M., 2020. Microemulsions as nano-reactors for the solubilization, separation, purification and encapsulation of bioactive compounds. Adv. Colloid Interface Sci. 283, 102227.
Jo, S., Lee, J.H., 2021. Evaluation of the effects of aldehydes on association colloid properties and oxidative stability in bulk oils. Food Chem. 338, 127778.
Jokar, M., Nateghi, L., Golmakani, M.T., Berenji, S., 2022. Effects of polyglycerol polyricinoleate on the antioxidant pathways of curcumin during the peroxidation of canola oil. Lwt 162, 113455.
Jorgensen, W.L., Maxwell, D.S., Tirado-Rives, J., 1996. Development and testing of the OPLS all-atom force field on conformational energetics and properties of organic liquids. J. Am. Chem. Soc. 118, 11225–11236.
Kamranfar, P., Jamialahmadi, M., 2014. Effect of surfactant micelle shape transition on the microemulsion viscosity and its application in enhanced oil recovery processes. J. Mol. Liq. 198, 286–291.
Kato, S., Shimizu, N., Hanzawa, Y., Otoki, Y., Ito, J., Kimura, F., Takekoshi, S., Sakaino, M., Sano, T., Eitsuka, T., et al., 2018. Determination of triacylglycerol oxidation mechanisms in canola oil using liquid chromatography–tandem mass spectrometry. npj Sci Food 2.
Kerrihard, A.L., Pegg, R.B., Sarkar, A., Craft, B.D., 2015. Update on the methods for monitoring UFA oxidation in food products. Eur. J. Lipid Sci. Technol. 117, 1–14.
Kittipongpittaya, K., Panya, A., McClements, D.J., Decker, E.A., 2014. Impact of free fatty acids and phospholipids on reverse micelles formation and lipid oxidation in bulk oil. JAOCS, J Am Oil Chem Soc 91, 453–462.
Kittipongpittaya, K., Panya, A., Decker, E.A., 2016. Role of water and selected minor components on association colloid formation and lipid oxidation in bulk oil. JAOCS, J Am Oil Chem Soc 93, 83–91.
Kortenska, V.D., Yanishlieva, N.V., Kasaikina, O.T., Totzeva, I.R., Boneva, M.I., Russina, I.F., 2002. Phenol antioxidant efficiency in various lipid substrates containing hydroxy compounds. Eur. J. Lipid Sci. Technol. 104, 513–519.
Mata, J., Varade, D., Bahadur, P., 2005. Aggregation behavior of quaternary salt based cationic surfactants. Thermochim. Acta 428, 147–155.
Mehta, B.M., Darji, V.B., Aparnathi, K.D., 2015. Comparison of five analytical methods for the determination of peroxide value in oxidized ghee. Food Chem. 185, 449–453.
Merkx, D.W.H., Hong, G.T.S., Ermacora, A., Van Duynhoven, J.P.M., 2018. Rapid quantitative profiling of lipid oxidation products in a food emulsion by 1H NMR. Anal. Chem. 90, 4863–4870.
Moradi, S., Nowroozi, A., Shahlaei, M., 2019. Shedding light on the structural properties of lipid bilayers using molecular dynamics simulation: a review study. RSC Adv. 9, 4644–4658.
Moultos, O.A., Tsimpanogiannis, I.N., Panagiotopoulos, A.Z., Trusler, J.P.M., Economou, I.G., 2016. Atomistic molecular dynamics simulations of carbon dioxide diffusivity in n -hexane, n -decane, n -hexadecane, cyclohexane, and squalane. J. Phys. Chem. B 120, 12890–12900.
Neff, W.E., Mounts, T.L., Rinsch, W.M., Konishi, H., El-Agaimy, M.A., 1994. Oxidative stability of purified canola oil triacylglycerols with altered fatty acid compositions as affected by triacylglycerol composition and structure. J. Am. Oil Chem. Soc. 71, 1101–1109.
Nguyen, K.A., Hennebelle, M., van Duynhoven, J.P.M., Dubbelboer, A., Boerkamp, V.J. P., Wierenga, P.A., 2024. Mechanistic kinetic modelling of lipid oxidation in vegetable oils to estimate shelf-life. Food Chem. 433, 137266.
Packwood, D.M., Han, P., Hitosugi, T., 2017. Chemical and entropic control on the molecular self-assembly process. Nat. Commun. 8, 1–8.
Paradiso, V.M., Pasqualone, A., Summo, C., Caponio, F., 2018. An "omics" approach for lipid oxidation in foods: the case of free fatty acids in bulk purified olive oil. Eur. J. Lipid Sci. Technol. 120, 1–10.
Pehlivanoglu, H., Demirci, M., Toker, O.S., 2018. Rheological properties of wax oleogels rich in high oleic acid. Int. J. Food Prop. 20, S2856–S2867.
Priyanto, S., Mansoori, G.A., Suwono, A., 2001. Measurement of property relationships of nano-structure micelles and coacervates of asphaltene in a pure solvent. Chem. Eng. Sci. 56, 6933–6939.
Qiao, B., Demars, T., Olvera De La Cruz, M., Ellis, R.J., 2014. How hydrogen bonds affect the growth of reverse micelles around coordinating metal ions. J. Phys. Chem. Lett. 5, 1440–1444.
Sagalowicz, L., Leser, M.E., Watzke, H.J., Michel, M., 2006. Monoglyceride self-assembly structures as delivery vehicles. Trends Food Sci. Technol. 17, 204–214.
Schaich, K.M., 2020. Lipid oxidation: new perspectives on an old reaction. Bailey's Ind Oil Fat Prod. https://doi.org/10.1002/047167849X.BIO067.PUB2.
Siani, P., de Souza, R.M., Dias, L.G., Itri, R., Khandelia, H., 2016. An overview of molecular dynamics simulations of oxidized lipid systems, with a comparison of ELBA and MARTINI force fields for coarse grained lipid simulations. Biochim. Biophys. Acta Biomembr. 1858, 2498–2511.
Smith, A., 2022. An Overview of Molecular Dynamics Simulation for Food Products and Processes.
Velasco, J, Dobarganes, C, 2002. Oxidative stability of virgin olive oil. Eur. J. Lipid Sci. Technol. 104, 661–676.
Wang, X., Chen, Y., McClements, D.J., Meng, C., Zhang, M., Chen, H., Deng, Q., 2024. Recent advances in understanding the interfacial activity of antioxidants in association colloids in bulk oil. Adv. Colloid Interface Sci. 325, 103117.
Wu, C., Li, N.J., Chen, K.C., Hsu, H.F., 2014. Determination of critical micelle concentrations of ionic and nonionic surfactants based on relative viscosity measurements by capillary electrophoresis. Res. Chem. Intermed. 40, 2371–2379.
Yadav, D.K., Kumar, S., Choi, E.H., Chaudhary, S., Kim, M.H., 2019. Molecular dynamic simulations of oxidized skin lipid bilayer and permeability of reactive oxygen species. Sci. Rep. 9, 1–10.
Zlatkevich, L., 2002. Various procedures in the assessment of oxidation parameters from a sigmoidal oxidation curve. Polym. Test. 21, 531–537.